

Supporting Information

3D Biomimetic Tongue-Emulating Surfaces for Tribological Applications

**Efren Andablo-Reyes¹, Michael Bryant², Anne Neville², Paul Hyde³, Rik Sarkar⁴,
Mathew Francis¹, and Anwasha Sarkar^{1*}**

¹Food Colloids and Bioprocessing Group, School of Food Science and Nutrition, University of Leeds, Leeds, LS2 9JT, UK

²Institute of Functional Surfaces, School of Mechanical Engineering, University of Leeds, Leeds, LS2 9JT, UK

³School of Dentistry, University of Leeds, Leeds, LS2 9JT, UK

⁴School of Informatics, University of Edinburgh, Edinburgh, EH8 9AB, UK

Corresponding Author e-mail: A.Sarkar@leeds.ac.uk

CONTENT

S1. Topographic analysis of selected areas of human tongue surface.

S2. Material characteristics of pig's tongue.

S3. Electron micrographs of soft hydrophilic polymeric tongue and 3D printed tongue-like surfaces.

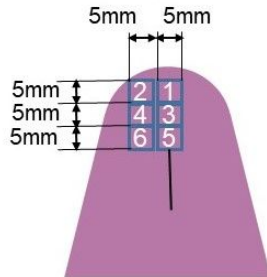
S4. Rheology and tribology of model hydrophilic lubricants.

S5. Positive 3D optical scan and surface reconstruction of polymeric surfaces before and after tribological testing.

S6. Adsorption behaviour of whey protein and xanthan gum on PDMS surfaces.

S1. Topographic analysis of selected areas of human tongue surface.

Table S1| Topographic analysis of selected areas of a human tongue surface. Roughness parameters S_a , S_q , S_p and S_v calculated from negative tongue impressions (n = 15) using either hydrophobic (polyvinyl siloxane) or hydrophilic (alginate) masks ((Ethics DREC ref: 120318/AS/245, University of Leeds). Roughness is measured in six different regions near the tip as depicted in the schematic of the human tongue provided on the left of the table.



Zone	Polyvinyl siloxane (Hydrophobic)				Alginate (Hydrophilic)			
	S_a	S_q	S_p	S_v	S_a	S_q	S_p	S_v
1	119 +/- 28	153 +/- 33	519 +/- 111	460 +/- 66	118 +/- 53	150 +/- 68	440 +/- 144	463 +/- 190
2	119 +/- 38	148 +/- 40	491 +/- 52	477 +/- 118	106 +/- 36	134 +/- 43	399 +/- 114	457 +/- 138
3	121 +/- 65	154 +/- 75	453 +/- 154	510 +/- 207	112 +/- 23	143 +/- 27	433 +/- 85	439 +/- 92
4	120 +/- 47	150 +/- 56	483 +/- 144	511 +/- 184	94 +/- 30	121 +/- 38	422 +/- 140	392 +/- 128
5	142 +/- 64	174 +/- 71	522 +/- 216	498 +/- 159	103 +/- 24	132 +/- 29	458 +/- 179	523 +/- 87
6	111 +/- 47	142 +/- 59	529 +/- 203	494 +/- 233	83 +/- 12	105 +/- 13	338 +/- 85	375 +/- 81

S2. Material characteristics of pig's tongue.

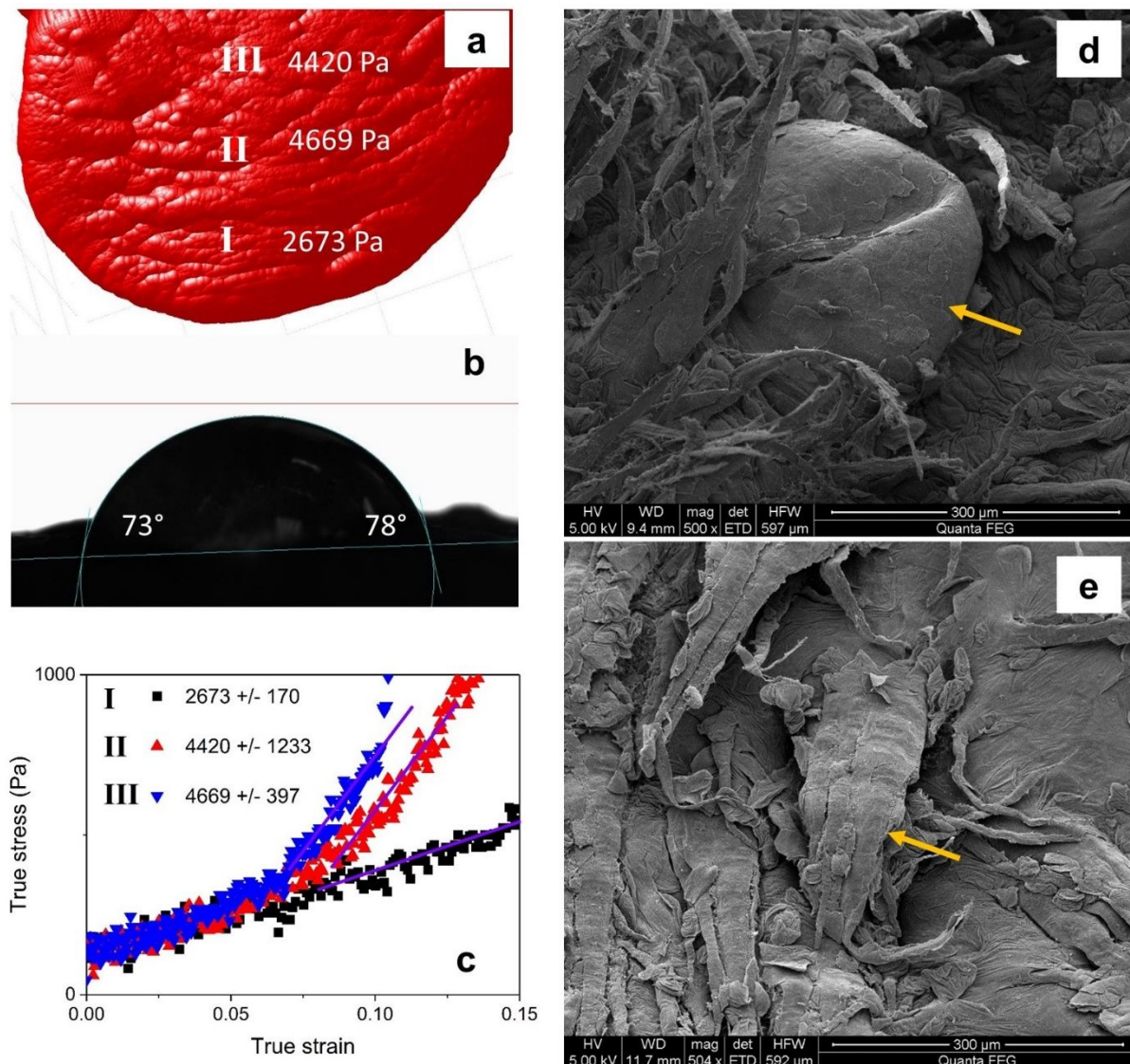


Figure S1| Material characteristics of a pig tongue. (a) 3D-laser scanning of a pig tongue (collected within 2 hours of sacrifice of the pig's tongue) showing the dorsal anterior section and the Young's modulus at each of the parts derived from (c). (b) Wettability measurements on the air-dried pig tongue surface using sessile drop method. (c) Single compression test performed on the air-dried tongue using TA-TX2 texture analyser. Young modulus is calculated as the slope of the linear fitting of the stress vs strain curves. Compression test were performed on 1 cm diameter cylinders obtained for different sections of the pig tongue as shown in (a). Scanning electron microscopy images of fungiform (d) and filiform (e) papilla respectively, shown by yellow arrows, on the dorsal anterior section. Papillae of the pig's tongue has a similar shape to human counterparts, however papillae of pig's tongue is about half the size of their human counterparts (refer to **Figure 1c** for human tongue papillae).

S3. Electron micrographs of soft hydrophilic polymeric tongue and 3D printed tongue-like surfaces.

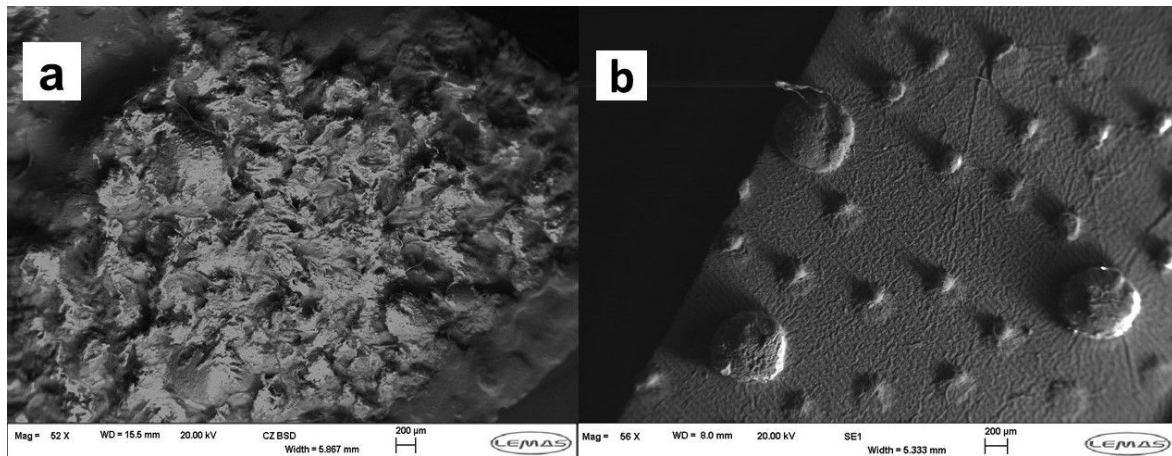


Figure S2| Electron micrographs of a soft hydrophilic polymeric tongue and 3D-printed tongue-like surfaces. Scanning electron microscopy images of surfaces **(a)** Ecohl tongue *i.e.* hydrophilic Ecoflex™ 0030 surface created by replica-moulding using polyvinyl siloxane negative surfaces obtained using real human tongue surface ((Ethics DREC ref: 120318/AS/245, University of Leeds) and **(b)** Ecohlprint *i.e.* hydrophilic Ecoflex™ 0030 + Span 80 surface made by 3D printing of surface created using a Poisson point process to obtain a random distribution of papillae and treatment with Span 80 before polymer crosslinking. Surfaces were coated with a thin film of gold (~ 10.0 nm) for correct imaging during scanning electron microscopy. Imaging was performed using a voltage of 20.0 kV.

S4. Rheology and tribology of model hydrophilic lubricants.

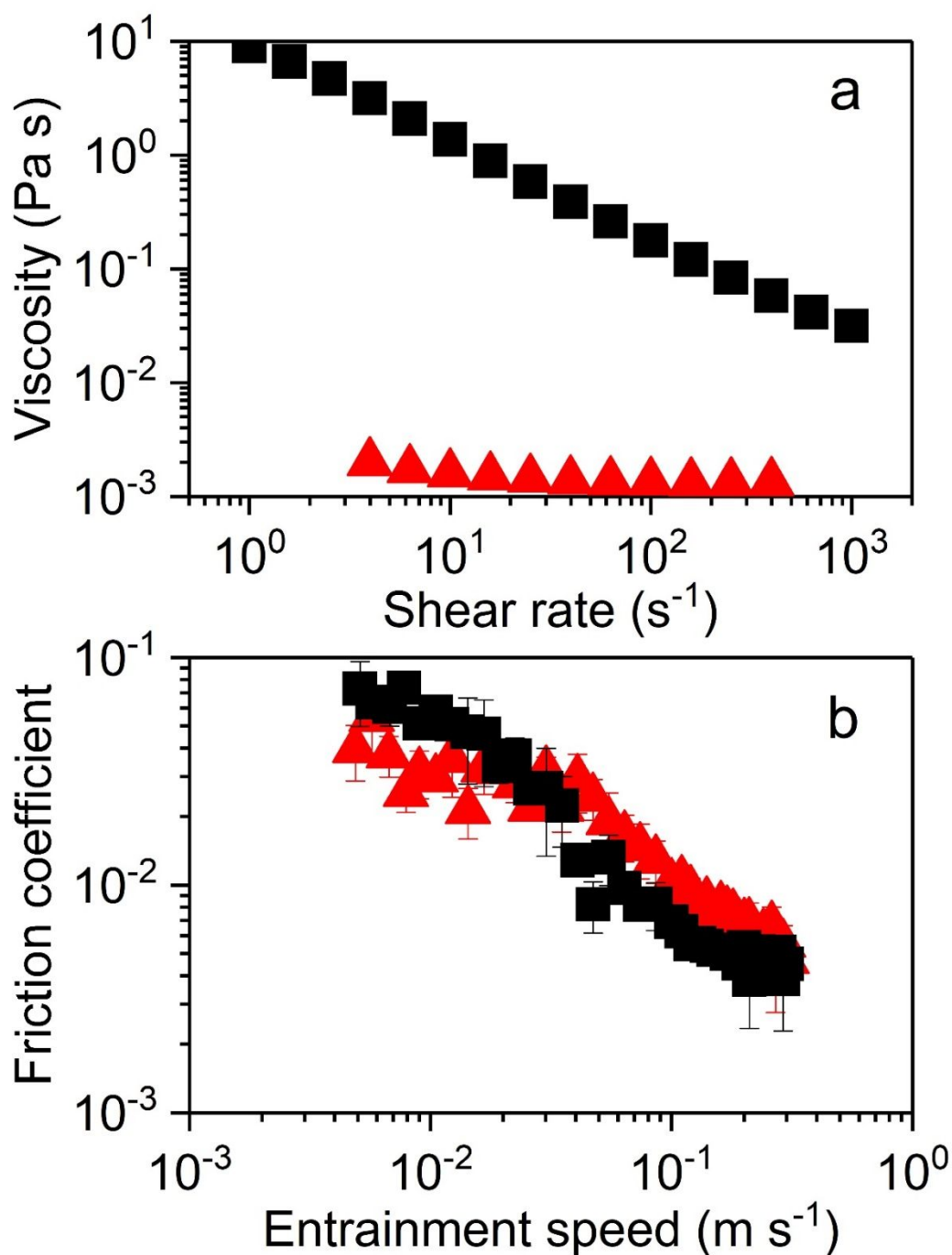


Figure S3| Rheology and tribology of model hydrophilic lubricants. (a) Flow curves and **(b)** friction coefficients versus entrainment speed of 1.0 wt% xanthan gum solution (■) and 10.0 wt% whey protein solution (▲). Despite having significantly different viscosities in **(a)**, their tribological performance in **(b)** is very similar. The tribology experiments in **(b)** were carried out using a smooth hydrophobic polydimethylsiloxane (PDMS) surface of 50 nm surface roughness which is considered as the current state-of-the-art for oral tribological testing.

S5. Positive 3D optical scan and surface reconstruction of polymeric surfaces before and after tribological testing.

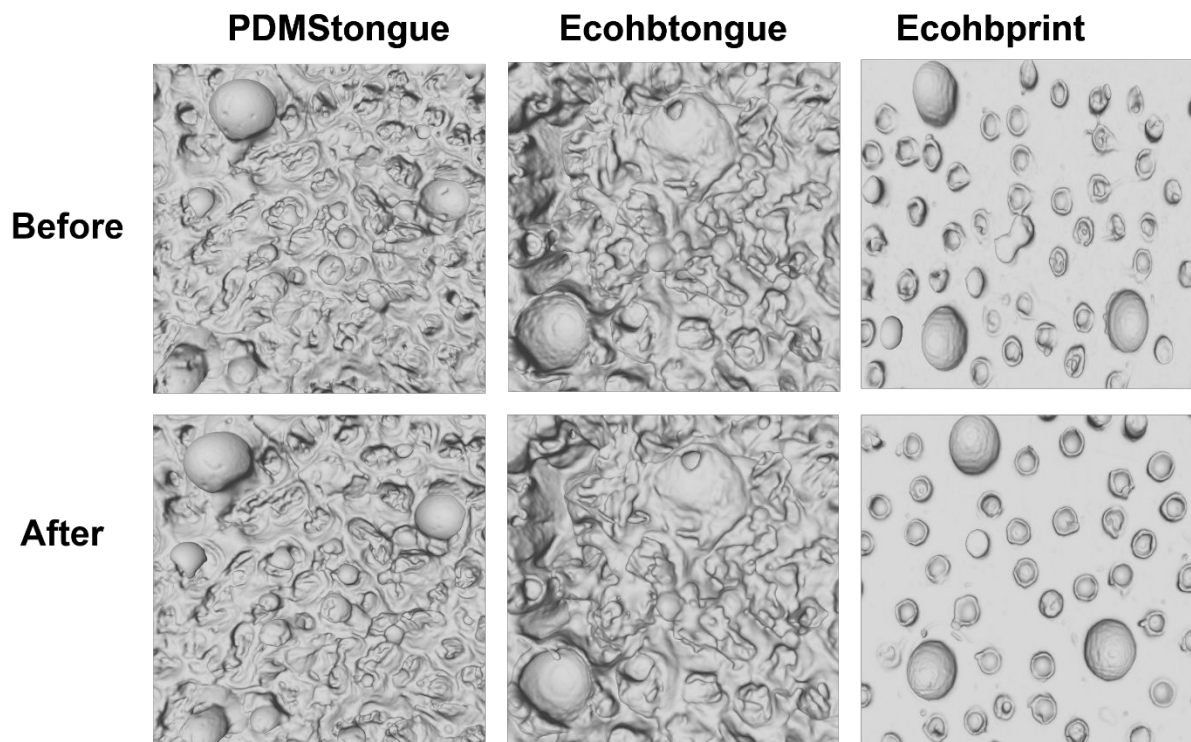


Figure S4| Positive 3D optical scan and surface reconstruction of polymeric surfaces before and after tribological testing. Surfaces generated using Screened Poisson surface reconstruction of the point datasets obtained from the 3D optical scanning before and after the mechanical friction developed during the tribological testing of different model hydrophilic lubricants under a pressure of 2.5 kPa. Surfaces do not show any signs of wear.

S6. Adsorption behaviour of whey protein and xanthan gum on PDMS surfaces.

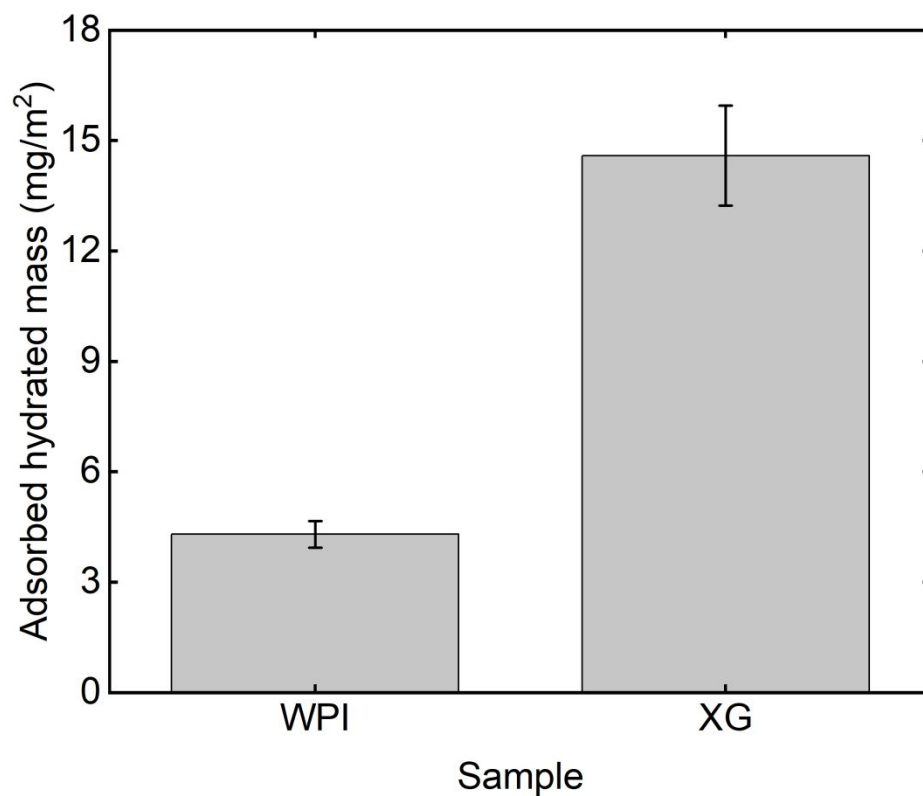


Figure S5| Hydrated mass of whey protein isolate (WPI) and xanthan gum (XG). The hydrated mass of whey protein (WPI) was three-times lower than that of xanthan gum on hydrophobic PDMS-coated sensors obtained using quartz crystal microbalance with dissipation monitoring (QCM-D).